Surface Review and Letters, Vol. 9, No. 2 (2002) 877–881

MAGNETIC MICROSPECTROSCOPY BY A COMBINATION OF XMCD AND PEEM

S. IMADA and S. SUGA
Graduate School of Engineering Science, Osaka University, 1-3 Machikaneyama, Toyonaka 560-8531, Japan

W. KUCH and J. KIRSCHNER
Max-Planck-Institut für Mikrostrukturphysik, Weinberg 2, D-06120 Halle, Germany

The benefits of combining soft X-ray magnetic circular dichroism and photoelectron microscopy are demonstrated by applying this combination (XMCD–PEEM) not only to magnetic domain imaging but also to quantitative evaluation of the distribution of spin and orbital magnetic moments. The latter takes full advantage of the spectroscopic aspect of XMCD–PEEM.

1. Introduction

The study of magnetic nanostructures has been attracting considerable attention as one of the most important fields in nanotechnology. It has become necessary not only to observe magnetic domains and their response to applied magnetic fields, but also to evaluate magnetic properties, on a microscopic scale. Observation of X-ray magnetic circular dichroism (XMCD) for core-level absorption of magnetic materials is a well-known tool for estimating spin and orbital magnetic moments in an element-specific manner. By combining photoelectron emission microscopy (PEEM) with XMCD, submicron resolution can be achieved.[1]

In this paper, we present applications of the combination of XMCD and PEEM (XMCD–PEEM) not only to magnetic domain imaging but also to quantitative evaluation of the distribution of spin and orbital magnetic moments. In Sec. 2, we introduce the principles of XMCD–PEEM by describing XMCD first and then XMCD–PEEM. In Sec. 3, the experimental setup is explained. In Sec. 4, the behavior of magnetic domain structures of triangular magnetic microstructures is presented. Finally, in Sec. 5, a spin reorientation transition is investigated by truly taking advantage of the spectroscopic aspect of XMCD–PEEM.

2. Principles of XMCD–PEEM

2.1. *XMCD and its origin*

The absorption intensity of circularly polarized soft X-rays by a ferromagnetic material is different between parallel and antiparallel orientations of the magnetization direction and the photon spin.[2,3] This phenomenon is called soft X-ray magnetic circular dichroism (XMCD). Since in the soft X-ray region, one can utilize absorption edges due to the electronic excitation from core levels to the empty states, XMCD has a powerful characteristic, namely the element selectivity.

Strong XMCD is seen, for example, in the $2p$ absorption spectrum ($2p$-XAS) of Fe. This $2p$-XAS is caused by the excitation of the $2p$ electrons of Fe to the $3d$ conduction band. As a model case, let us suppose, as in Fig. 1(a), that circularly polarized soft X-rays with the photon spin of $\mu = +1$ are incident on to the sample in a negligibly small grazing angle. In this case, the magnetization direction of region I (II) is parallel (antiparallel) to the photon spin.

Consider the spin angular momentum of the Fe $3d$ electrons, whose direction is antiparallel to the magnetization. Since the directions of the majority spin of regions I and II are downward ($\downarrow$) and upward ($\uparrow$), respectively, the $3d$ band structure of the two regions can be illustrated by Figs. 1(b) and 1(c).

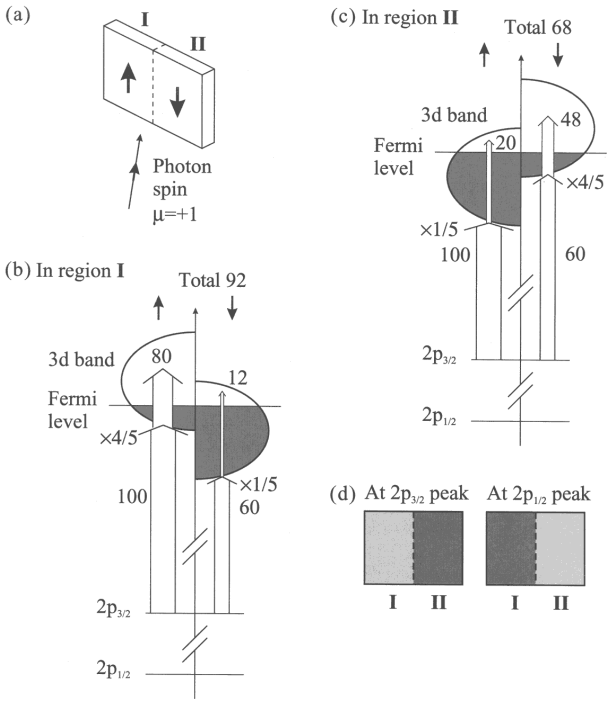

Fig. 1. Principle of XMCD. (a) A model of experimental geometry. (b), (c) Probabilities of transition from $2p_{3/2}$ to $3d$ ferromagnetic band. (d) Resultant XMCD contrast.

To make the following discussion simple, we assume that the occupancies of majority and minority spin bands are 4/5 and 1/5, respectively.

The $2p$ core level of Fe is split into two levels, namely $2p_{3/2}$ with total angular momentum $j = 3/2$ and $2p_{1/2}$ with $j = 1/2$, due to a large spin–orbit interaction. In the $j = 3/2$ (1/2) state, spin and orbital angular momenta couple parallel (antiparallel) to each other. We can take advantage of the energy difference between these levels and excite electrons from only one of the two levels into the $3d$ orbital.

Due to the selection rule, the circularly polarized photons with upward photon spin [see Fig. 1(a)] preferentially excite $2p$ electrons with upward orbital angular momentum into the $3d$ level. An additional effect of the spin–orbit interaction is that, from the $2p_{3/2}$ ($2p_{1/2}$) level, an electron with spin of the same (opposite) direction as the orbital angular momentum, namely a $\uparrow$ ($\downarrow$) electron, is likely to be excited.[4] After simple calculations and taking the transition probability of $\uparrow$ electron from the $2p_{3/2}$ to be 100, that for $\downarrow$ electron of $2p_{3/2}$ is 60, and that for $\uparrow$ ($\downarrow$) $2p_{1/2}$ electron is 20 (60).

Now, electrons excited from the $2p$ core level cannot move into any of the occupied sates. For example, in region I, the allowed transition probability is $100 \times 4/5 = 80$ for $\uparrow$ electrons and $60 \times 1/5 = 12$ for $\downarrow$ electrons, the sum being 92 [see Fig. 1(b)]. For region II, the allowed transition probability is in total 68 [see Fig. 1(c)]. Since the photoabsorption intensity is proportional to the probability of the allowed transition, the $2p_{3/2} \rightarrow 3d$ absorption intensity ratio between regions I and II is 92 : 68 in this model. For $2p_{1/2} \rightarrow 3d$, the absorption intensity ratio is 28 : 52. Therefore, as shown in Fig. 1(d), where the lighter part represents larger XAS, the $2p_{3/2} \rightarrow 3d$ ($2p_{1/2} \rightarrow 3d$) absorption is stronger in the region that is magnetized in the same (opposite) direction as the photon spin.

Numerical analysis of the XMCD spectrum leads to quantitative information about the spin magnetic moment and the orbital magnetic moment. This is based on the sum rules proposed by Thole *et al.*[5] and Carra *et al.*,[6] which yield $\langle M_S \rangle$ and $\langle M_L \rangle$, the projections of spin magnetic moment $-2\mathbf{S}$ and orbital magnetic moment $-\mathbf{L}$ on the quantization axis, from the XAS spectra for circularly polarized photons with photon spin parallel (I_+) and antiparallel (I_-) to the quantization axis and the XAS spectrum for linearly polarized photons with electric vector parallel to the quantization axis (I_0). For example, for the $2p \rightarrow 3d$ XAS of transition metals, the sum rules can be written as

$$\langle M_L \rangle = 2\frac{\int d\varepsilon(I_+ - I_-)}{\int d\varepsilon(I_+ + I_- + I_0)} \tag{1}$$

and

$$\langle M_S \rangle = 3\frac{\int_{j=3/2} d\varepsilon(I_+ - I_-) - 2\int_{j=1/2} d\varepsilon(I_+ - I_-)}{\int d\varepsilon(I_+ + I_- + I_0)}, \tag{2}$$

if the magnetic dipole operator is neglected. In this paper, we replace I_0 with the average of I_+ and I_- for simplicity, which is a good approximation so long as the magnetic anisotropy is not too large.

2.2. *XMCD microspectroscopy — PEEM and transmission methods*

In XMCD microspectroscopy, one magnifies and observes the microscopic distribution of XMCD on a sample. One way is to magnify the transmitted soft X-rays by using a zone plate.[7] Another way is to magnify the emitted photoelectrons by using an

electron microscope.[1] A merit of the latter, which we utilize in this paper, is that it can be applied for a sample grown on a thick substrate that soft X-rays would not penetrate. We should also note the merit of the former; namely, that observation can be carried out even in applied magnetic fields since it is a photon-in photon-out measurement.

The electron microscope that is used in XMCD microspectroscopy is called a photoelectron emission microscope (PEEM). In a PEEM, electrons emitted from the sample are projected on a fluorescent screen by electron lenses. When used in XMCD microspectroscopy, PEEM is set to observe the secondary electrons emitted as a consequence of the absorption of soft X-rays. It is known that the intensity of the secondary electrons depends approximately linearly upon the photoabsorption intensity. Therefore, by observing a PEEM image, the distribution of the XAS intensity can be observed.

3. Experiment

The measurements were performed at the twin helical undulator beamline for soft X-ray spectroscopy BL25SU of SPring-8 in Japan.[8] The photon spin was chosen by closing one undulator and fully opening the other. The light was incident on to the sample at a grazing angle of 30° from the surface. The setup of the photoemission microscope (Focus IS-PEEM) was identical to that described in previous publications.[9] By setting the contrast aperture to 70 μm and the extractor voltage to 10 kV, a field of view of about 50–100 μm and a lateral resolution of about 0.4 μm were achieved.

4. Magnetic Domains of a Triangular Microstructure

We have investigated the effect of magnetic field pulses on the domain structures of triangular microstructures by means of XMCD–PEEM. Samples were microstructures of 30-nm-thick polycrystalline Co film made on a Si substrate by electron beam lithography and the liftoff technique.

In order to improve the magnetic contrast, we took PEEM images at two photon energies corresponding to Co $2p_{3/2}$ and $2p_{1/2} \rightarrow 3d$ transitions with the same photon spin and generated an asymmetry image. This image is the distribution of the asymmetry $A \equiv [I(2p_{3/2}) - I(2p_{1/2})]/[I(2p_{3/2}) + I(2p_{1/2})]$, which depends linearly on the projection of the magnetic moment on the photon spin. The pulsed magnetic field for magnetization was applied along the in-plane direction, i.e. parallel to the surface, by discharging a capacitor through a coreless solenoidal coil, and measurement was carried out under zero field.

The transformation of the magnetic domains caused by a series of magnetic field pulses is summarized in Figs. 2 and 3. In these figures, circularly polarized light of photon spin $\mu = +1$ was incident on to the sample from the bottom to the top in the figure. Therefore, the lightest part of the image, corresponding to the largest asymmetry A, is magnetized in the upward direction and the darkest part is magnetized in the downward direction. The regions with the medium contrast, found mainly near the top edge of the triangle, are magnetized to the right or left direction. The region near an edge of the triangle is magnetized along a direction parallel to the edge. The total magnetization projected on to the direction of the photon spin in each state was estimated by integrating the asymmetry A over the whole triangle. The direction of the pulsed magnetic field was nearly parallel to the photon spin;

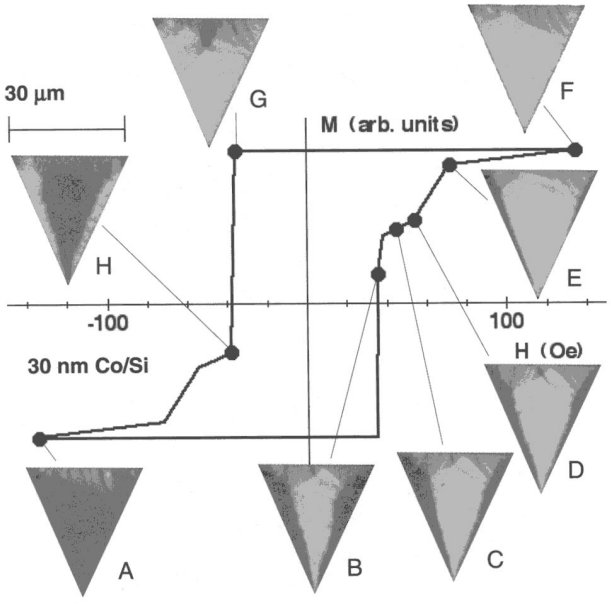

Fig. 2. Transformation of the magnetic domain structure of the triangular Co microstructure by magnetic field pulses, corresponding to a major hysteresis loop.

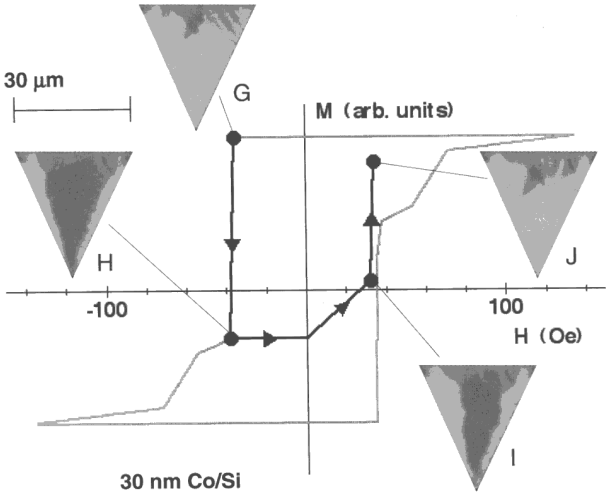

Fig. 3. The same as in Fig. 2 but for a minor hysteresis loop.

namely, positive magnetic field $H > 0$ corresponds to an upward magnetic field.

In Fig. 2 is shown the transformation corresponding to the major hysteresis loop. Namely, the direction of the magnetic field is reversed only after saturation is achieved. However, we should note that the "hysteresis loop" drawn here is not a hysteresis loop in the normal sense since, here, the image, and therefore also the magnetization, are those under zero field after applying the magnetic field pulse. Starting from a saturated domain structure as in images A and F, magnetic field pulses of the opposite direction with increasing magnitude were applied. The magnetization reversal process is revealed to start with the nucleation of a small magnetic domain near the top edge, as seen in image G. Next, this domain grows downward until it touches the bottom apex as in images H and B. By increasing the magnitude of the magnetic field pulses, the magnetic domain in the center gradually expands to both sides, as seen in images C, D and E. By applying a sufficiently large magnetic field, the domains with the other magnetization direction in both sides are wiped out, leaving some regions not saturated near the top edge, as in images A and F.

Figure 3 shows the transformation of the domain structure corresponding to a minor hysteresis loop. After a downward magnetized domain was made in the central part as in image H by downward magnetic field pulses, upward pulses were applied. Then, as shown in images I and J, the area of the upward magnetized domain in the both sides increased, instead of a new upward magnetized domain generated near the top edge. The contrast is totally opposite between, for example, images I and B, although they are at about the same position in the $H - M$ space. This topological contrast is interpreted to be connected to the difference between the major and minor hysteresis loops.

5. Spin Reorientation Transition in an Epitaxial Co/Ni Bilayer

The study of magnetization easy directions is quite important in the field of magnetic thin films and superstructures. At room temperature, by increasing the thickness of the epitaxially grown Ni film on Cu(001), the magnetization easy axis changes from in-plane to out-of-plane at around 10 monolayers (ML) and then again to in-plane at around 60–70 ML. Furthermore, evaporation of a few monolayers of Co on top of the Ni film in the out-of-plane thickness region makes the easy axis in-plane.[10,11]

In order to study the mechanism of this spin reorientation transition, a crossed double-wedged Co/Ni/Cu(001) was prepared. Namely, Ni was evaporated on Cu(001) in a wedge shape with the thickness varying in the x direction in the range of 0–14 ML, on top of which 0–4 ML Co was evaporated whose thickness was varied in the y direction. The sample was intentionally not magnetized neither during nor after the sample preparation.

In order to use the XMCD sum rules described in Subsec. 2.1, Eqs. (1) and (2), PEEM images were taken for each photon spin at 105 photon energy points between 845 eV and 890 eV, which covers the Ni $2p_{3/2}$ and $2p_{1/2}$ photoabsorption regions. Since each image consisted of $192 \times 200 = 38{,}400$ pixels, this yields 38,400 sets of I_+ and I_- spectra.

Figure 4 shows the distribution of M_S, whose quantization axis is the incident direction of the soft X-ray, pointing to the y axis of the figure with an angle of 30° from the sample surface. The whole area can be divided into two by the dotted white line, above which are four levels of contrast and below which are only two levels. When Ni is magnetized in the plane, the magnetization easy directions are the four directions equivalent to [110] shown in the lower right hand corner of the figure. Therefore, the four levels of contrast in the upper part correspond to

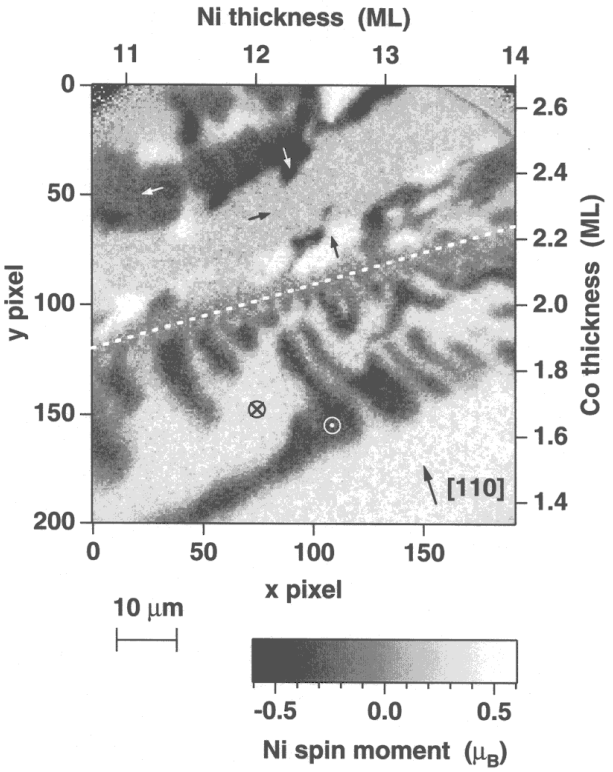

Fig. 4. Distribution of the Ni 3*d* spin magnetic moment for a Co/Ni/Cu(001) double wedge.

the four directions of magnetization shown by the arrows. On the other hand, the two levels in the lower part correspond to the two out-of-plane directions, one going into the sheet (⊗) and the other coming out of the sheet (⊙). The white dotted line corresponding to the spin reorientation transition line was approximately $d_{\mathrm{Co}} = 0.116\, d_{\mathrm{Ni}} + 0.62$, where d_{Co} and d_{Ni} are the thicknesses of Co and Ni in units of ML.

By combining Fig. 4 and the distribution of M_L (not shown here), it was found that the orbital magnetic moment changes its value between in-plane (0.034 μ_{B}) and out-of-plane (0.052 μ_{B}) magnetized phases, while the spin magnetic moment was about the same value of 0.65 μ_{B} for both phases. This suggests that the gain of the energy caused by the spin–orbit interaction is larger in the out-of-plane phase than in the in-plane phase, which is consistent with the fact that the magnetization easy direction of the Ni film alone is out-of-plane in this thickness range.

6. Summary

We demonstrated the capabilities of XMCD–PEEM through application to magnetic domain imaging and also to a quantitative mapping of the spin and orbital magnetic moments through microspectroscopy. By using the aspect of imaging, we have studied the transformation of the magnetization domain structure. We have shown the qualitative difference in the transformation of the domain structure between major and minor hysteresis loops. By taking advantage of the microspectroscopic aspect, we have studied the spin reorientation transition seen in a Co/Ni bilayer. It was shown that the orbital magnetic moment changes by about 30% at the transition while the spin magnetic moment stays about constant.

Acknowledgments

Experiments at SPring-8 were performed with the approval of the Japan Synchrotron Research Institute (JASRI) (proposal No. 1999A0319-NS-np). The study was done as a Japan–Germany collaboration project financially supported by the Japan Society for Promotion of Science and the Deutsche Forschungsgemeinschaft (Nos. Ki 358/3-1 and 446 JAP-113/179/0). The study was also supported by a Grant-in-Aid for COE Research (10CE2004) from the Ministry of Education, Science, Sports and Culture, Japan. We would like to thank K. Gamo, J. Yanagisawa and T. Kimura of Osaka University for providing the magnetic microstructured samples.

References

1. J. Stöhr *et al.*, *Science* **259**, 658 (1993).
2. G. Schütz *et al.*, *Phys. Rev. Lett.* **58**, 737 (1987).
3. C. T. Chen *et al.*, *Phys. Rev.* **B42**, 7262 (1990).
4. S. Imada and T. Jo, *J. Phys. Soc. Jpn.* **59**, 3358 (1990).
5. B. T. Thole *et al.*, *Phys. Rev. Lett.* **68**, 1943 (1992).
6. P. Carra *et al.*, *Phys. Rev. Lett.* **70**, 694 (1993).
7. P. Fischer *et al.*, *J. Phys.* **D31**, 649 (1998).
8. Y. Saitoh *et al.*, *J. Synchrotron Rad.* **5**, 542 (1998).
9. W. Kuch *et al.*, *Surf. Rev. Lett.* **5**, 1241 (1998).
10. H. A. Dürr *et al.*, *Science* **277**, 213 (1997).
11. S. van Dijken *et al.*, *J. Magn. Magn. Mater.* **210**, 316 (2000).